Mechanism and Optimization Method of Leakage Magnetic Field Reduction Using Active Shielding in Wireless Power Transfer

Kaito Takashima
Faculty of Science and Technology
Tokyo University of Science
Noda, Japan
takashima.kaito22@gmail.com

Takehiro Imura
Faculty of Science and Technology
Tokyo University of Science
Noda, Japan

Yoichi Hori
Faculty of Science and Technology
Tokyo University of Science
Noda, Japa

***Abstract*— Leakage magnetic field is one of the problems of wireless power transfer, which is now used in a variety of situations. Leakage magnetic fields are feared to have adverse effects on the human body and electronic devices and must be for reducing leakage magnetic fields. Passive shielding confines leakage magnetic fields with metal or magnetic materials. Active shielding counteracts leakage magnetic fields by using magnetic fields generated by shielding coils. In this paper, it is shown that the leakage magnetic field can be reduced by shifting the phase of the current flowing in the shielding coil from that of the transfer coil. And it is also shown that the optimum phase difference differs depending on the resonance method and the location of the shielding coil. Phase difference between transfer coil and shieling coil causes leakage magnetic field reduction. The influence of the phase difference between the transfer coil and the receiver coil, and between the shielding coil and the receiver coil is negligible. The phase difference is not necessarily the optimum one to be in the opposite phase. The case of a 600 V input to the transfer coil and a shielding coil installed next to the transfer coil or around the receiver coil is considered. In all cases of S-S, Double-LCC, and LCC-S, leakage magnetic fields can be reduced to about 1 mA/m by adjusting the phase difference between the transfer coil and the shielding coil. The reduction of leakage magnetic field by the phase difference and its optimum value are shown using the theoretical equation and electromagnetic field analysis using the method of moments.**

Keywords— ***Leakage Magnetic Field, Wireless Power Transfer, Reduction, EMF***

I. INTRODUCTION

Wireless power transfer, which transmits power to electronic devices without physical connection, is being used in a variety of situations. Wireless power transfer has been studied extensively in recent years because of its advantages such as improved positional freedom and compatibility due to the elimination of the need for a cable connection, and the possibility of reducing battery capacity. One of the challenges of this technology is leakage magnetic field. A leakage magnetic field is a magnetic field that does not contribute to power transfer and is generated in the surrounding area due to the current flowing in the coil during wireless power transfer by the magnetic field resonance method. Because of concerns about adverse effects on the human body and noise to peripheral devices, regulated values for the magnetic field strength are set by organizations such as SAE and CISPR[1][2]. In order to put wireless power transfer into practical use, leakage magnetic fields must be reduced below the regulated value.

The leakage magnetic field reduction methods proposed until now can be roughly classified into two types: passive shielding [3]-[8] and active shielding [9]-[10]. Active shielding is a method in which a magnetic field reducing coil including a power supply is added around the transfer coil and the leakage magnetic field is canceled by the magnetic field generated from the coil. This method can effectively reduce leakage magnetic fields. As shown in previous studies [9][10], the phase of the current flowing in the shielding coil is shifted from that of the transfer coil when the magnetic field is reduced by active shielding. Only the result that the leakage magnetic field is reduced by shifting the phase is shown, but the principle and the method of finding the optimum input voltage magnitude and phase difference are not mentioned.

In this paper, it is shown that the leakage magnetic field can be reduced by setting the input voltage phase to the shielding coil to an appropriate value in a situation where a transfer coil, a receiver coil, and a shielding coil are installed, using a mathematical formula. Phase difference between transfer coil and shielding coil causes leakage magnetic field reduction. The influence of the phase difference between the transfer coil and the receiver coil, and between the shielding coil and the receiver coil is negligible. It was also shown that the optimum input voltage to the shielding coil differs depending on the S-S, Double-LCC, and LCC-S resonance schemes of the circuit. The verification is performed by theoretical calculations and electromagnetic field analysis using the method of moments. Theoretical calculations were performed using only the coil design values and input voltages by converting the wireless power transfer system into an equivalent circuit. Although the electromagnetic field analysis is time-consuming and requires a powerful PC, the theoretical calculations can be performed on an ordinary notebook PC, which facilitates the system design.

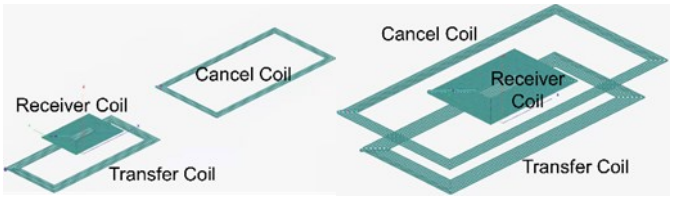

Fig.1 WPT system including shielding coil

II. Coil Configuration Under Consideration

The WPT system considered in this paper is shown in Fig. 1. The transfer coil is 1300 × 600 mm with 7 turns, the receiver coil is 580 × 420 mm with 16 turns, and the shielding coil is 1460 × 750 mm with 5 turns. The transmission distance is 200 mm and the load on the receiver coil is 10 Ω. The shielding coils are considered in two cases: one is placed next to the transfer coils and the other is placed around the receiver coils. Each coil is an air-core coil without aluminum or ferrite. The input voltage to the transfer coil is set to 600 V, and the input voltage to the shielding coil is set to the value that reduces the leakage magnetic field the most under each condition.

III. Theoretical Formula

A. Current

Current derivation is performed using the Double-LCC circuit as an example. Fig. 2 shows the equivalent circuit including the shieling coil. In Fig.2, the shielding coil is drawn next to the transfer coil. By changing the values of mutual inductances L_{ma} , L_{mb} and L_{mc} between the coils, the same equivalent circuit is obtained when the shielding coil is placed around the receiver coil. The mutual inductance is obtained from the Neumann equation (1). The parameters used are shown in Fig. 3.

$$L_m = \frac{\mu_0}{4\pi}\oint_{C_1}\oint_{C_2}\frac{dl_1 dl_2}{D} \tag{1}$$

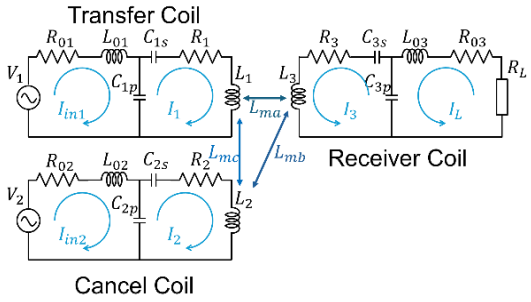

Fig.2 Double-LCC equivalent circuit

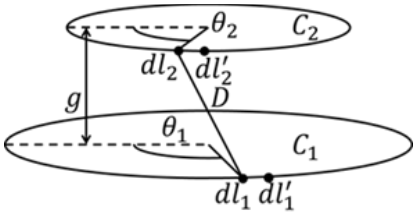

Fig.3 Parameters of the Neumann equation

The size of each capacitor is set as shown in equation (2) to reach resonance at 85 kHz.

$$\omega_0 = \frac{1}{\sqrt{L_{0x}C_{xp}}} = \sqrt{\frac{C_{xp}+C_{xs}}{L_x C_{xp} C_{xs}}}\,(x = 1,2,3) \tag{2}$$

Equation (3) is the circuit equation for each current in Fig. 2 and is expressed in matrix form.

$$\begin{bmatrix} V_1 \\ 0 \\ V_2 \\ 0 \\ 0 \\ 0 \end{bmatrix} = \begin{bmatrix} R_{01} & j\frac{1}{\omega C_{1p}} & 0 & 0 & 0 & 0 \\ j\frac{1}{\omega C_{1p}} & R_1 & 0 & j\omega L_{mt} & j\omega L_{ma} & 0 \\ 0 & 0 & R_{02} & j\frac{1}{\omega C_{2p}} & 0 & 0 \\ 0 & j\omega L_{mt} & j\frac{1}{\omega C_{2p}} & R_2 & j\omega L_{mb} & 0 \\ 0 & j\omega L_{ma} & 0 & j\omega L_{mb} & R_3 & j\frac{1}{\omega C_{3p}} \\ 0 & 0 & 0 & 0 & j\frac{1}{\omega C_{3p}} & R_{03}+R_L \end{bmatrix} \begin{bmatrix} I_{in1} \\ I_1 \\ I_{in2} \\ I_2 \\ I_3 \\ I_L \end{bmatrix} \tag{3}$$

By obtaining the inverse matrix of equation (3), each current can be obtained in complex number form. Therefore, it is possible to obtain the magnitude and phase of each current.

B. Magnetic Field

The leakage magnetic field strength is derived from the vector potential. The magnetic fields generated by the transfer coil L_1, adjacent transfer coil L_2 and receiver coil L_3 to an arbitrary point $P(x,y,z)$ shown in Fig.4 are represented by equations (4), (5), and (6) respectively. Here, the distances r_1, r_2 and r_3 to any point P are sufficiently longer than the lengths a_k, b_k, c_k, d_k, e_k and f_k of each side.

$$H_1 = \begin{Bmatrix} H_{1x} \\ H_{1y} \\ H_{1z} \end{Bmatrix} = \begin{cases} \frac{\sum_{k=1}^{n} a_k b_k}{4\pi}\frac{3xz}{r_1^5} I_1 \\ \frac{\sum_{k=1}^{n} a_k b_k}{4\pi}\frac{3yz}{r_1^5} I_1 \\ \frac{\sum_{k=1}^{n} a_k b_k}{4\pi}\frac{2z^2-x^2-y^2}{r_1^5} I_1 \end{cases} \tag{4}$$

$$H_2 = \begin{Bmatrix} H_{2x} \\ H_{2y} \\ H_{2z} \end{Bmatrix} = \begin{cases} \frac{\sum_{k=1}^{m} c_k d_k}{4\pi}\frac{3(x-x_2)(z-z_2)}{r_2^5} I_2 \\ \frac{\sum_{k=1}^{m} c_k d_k}{4\pi}\frac{3(y-y_2)(z-z_2)}{r_2^5} I_2 \\ \frac{\sum_{k=1}^{m} c_k d_k}{4\pi}\frac{2(z-z_2)^2-(x-x_2)^2-(y-y_2)^2}{r_2^5} I_2 \end{cases} \tag{5}$$

$$H_3 = \begin{Bmatrix} H_{3x} \\ H_{3y} \\ H_{3z} \end{Bmatrix} = \begin{cases} \frac{\sum_{k=1}^{l} e_k f_k}{4\pi}\frac{3x(z-g)}{r_3^5} I_3 \\ \frac{\sum_{k=1}^{l} e_k f_k}{4\pi}\frac{3y(z-g)}{r_3^5} I_3 \\ \frac{\sum_{k=1}^{l} e_k f_k}{4\pi}\frac{2(z-g)^2-x^2-y^2}{r_3^5} I_3 \end{cases} \tag{6}$$

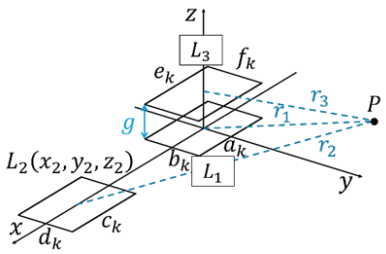

Fig.4 Parameters for magnetic field calculation

Since I_1, I_2 and I_3 have magnitude and phase, respectively, the equation (7) can be expressed as follows, where I_1, I_2 and I_3 are the magnitude and phase, respectively, and θ_1, θ_2 and θ_3 are the phase.

$$I_x = I_x \cos\theta_x + jI_x \sin\theta_x \quad (x = 1,2,3) \tag{7}$$

Note that I_x and θ_x can be expressed using the magnitude and phase of the input voltage and the coil design value from equation (3).

The magnitude of the magnetic field $\boldsymbol{H}$ at an arbitrary point P can be derived by composing H_1, H_2 and H_3. From equations (4), (5), (6), and (7), the magnitude of the magnetic field H can be expressed by equation (8).

$$H = \sqrt{\begin{matrix}(H_{1x}\cos\theta_1 + H_{2x}\cos\theta_2 + H_{3x}\cos\theta_3)^2 \\ +(H_{1x}\sin\theta_1 + H_{2x}\sin\theta_2 + H_{3x}\sin\theta_3)^2 \\ +\left(H_{1y}\cos\theta_1 + H_{2y}\cos\theta_2 + H_{3y}\cos\theta_3\right)^2 \\ +\left(H_{1y}\sin\theta_1 + H_{2y}\sin\theta_2 + H_{3y}\sin\theta_3\right)^2 \\ +(H_{1z}\cos\theta_1 + H_{2z}\cos\theta_2 + H_{3z}\cos\theta_3)^2 \\ +(H_{1z}\sin\theta_1 + H_{2z}\sin\theta_2 + H_{3z}\sin\theta_3)^2\end{matrix}} \tag{8}$$

C. Validation

The validity of equation (3)(8) is confirmed by comparison with electromagnetic field analysis. In the Double-LCC circuit, 600 V is applied to the transfer coil and 562 V is applied to the shielding coil. The comparison is made when the phase of the input voltage to the shielding coil is changed. The magnetic field intensity is measured at $(x, y, z) = (0, 11.9\ \text{m}, 1\ \text{m})$. Fig.5 and Fig.6 show the comparison results of current and magnetic field strength, respectively. Fig.5 and Fig.6 show that the current and magnetic field intensity are obtained with sufficient accuracy. Similar results were also obtained for other resonance methods..

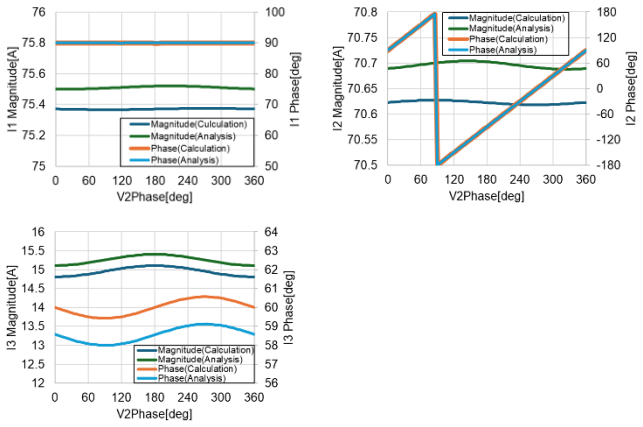

Fig.5 Current

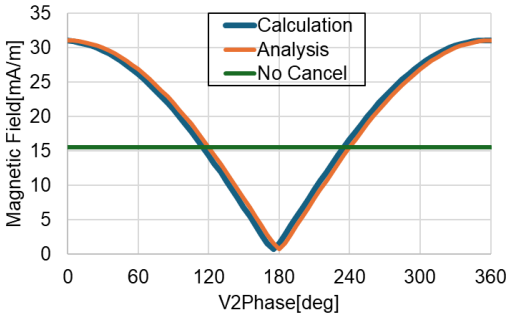

Fig.6 Magnetic field strength
(Double-LCC , shielding coil next to transfer coil)

IV. Mechanism of Leakage Magnetic Field Reduction

A. Explanation using theoretical formula

From IIIC, it can be confirmed that the magnetic field strength can be calculated using equation (8). Equation (8) shows that the magnetic field intensity is the sum of the magnetic fields generated by the three coils, but it is not clear how the magnetic field reduction occurs. Therefore, it is necessary to verify how the magnetic field reduction occurs by expanding equation (8). Equation (9) is the result of expanding equation (8).

$$H = \sqrt{\begin{matrix}H_{1x}^2 + H_{2x}^2 + H_{3x}^2 + H_{1y}^2 + H_{2y}^2 + H_{3y}^2 + H_{1z}^2 + H_{2z}^2 + H_{3z}^2 \\ +2\left(H_{1x}H_{2x} + H_{1y}H_{2y} + H_{1z}H_{2z}\right)\cos(\theta_1 - \theta_2) \\ +2\left(H_{1x}H_{3x} + H_{1y}H_{3y} + H_{1z}H_{3z}\right)\cos(\theta_1 - \theta_3) \\ +2\left(H_{2x}H_{3x} + H_{2y}H_{3y} + H_{2z}H_{3z}\right)\cos(\theta_2 - \theta_3)\end{matrix}} \tag{9}$$

Equation (9) shows that the current phase difference between the transfer coil, the receiver coil, and the shielding coil affects the total magnetic field strength. Equation (3) shows that these phase differences change as the input voltage phase to the shielding coil is changed. Then, compare the magnitudes of the first, second, third, and fourth terms in the root sign of equation (9), starting from the top.

B. Result of decomposing each term

1) Double-LCC circuit

In the Double-LCC circuit, the magnitude of each term is shown in Fig. 7 when the shielding coil is installed next to the transfer coil. The input voltage to the transfer coil is 600 V and that to the shielding coil is 562 V.

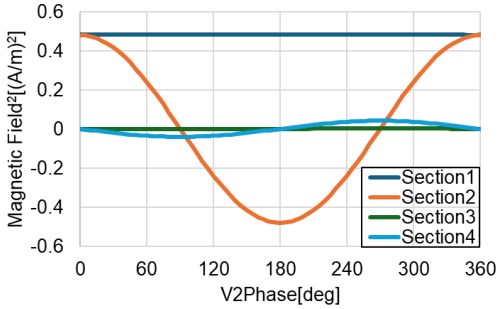

Fig.7 Comparison of magnitude for each term
(Double-LCC , Shielding coil next to transfer coil)

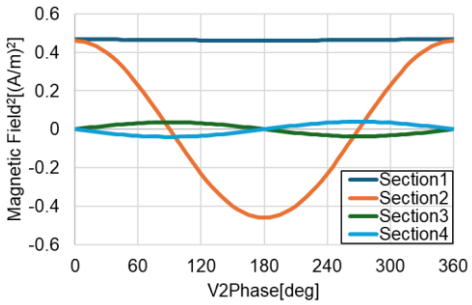

Fig.8 Comparison of the magnitude of each term
(Double-LCC, Shielding coil around receiver coil)

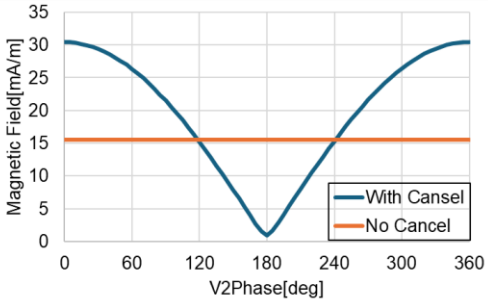

Fig.9 Magnetic field strength
(Double-LCC, Shielding coil around receiver coil)

From Fig.7, the changes of the first, third, and fourth terms are small. The first term doesn't include the phase difference component. The third term includes the current phase difference between the transfer coil and the receiver coil. The fourth term includes the current phase difference between the shielding coil and the receiver coil. On the other hand, the value of the second term changes to a large negative value. The second term includes the current phase difference between the transfer coil and the shielding coil. Since the second term changes significantly with the change of the input voltage phase to the shielding coil, it is found to be more dominant than the other terms. Therefore, it can be said that the second term is responsible for the magnetic field reduction effect. The leakage magnetic field is reduced the most when the phase of the input voltage to the shielding coil is 180 deg, where the second term is the smallest, as seen in the total magnetic field intensity from Fig.6. Fig.8 shows the magnitude of each term and Fig.9 shows the total magnetic field intensity when the shielding coil is installed around the receiver coil. The magnitude of the input voltage to the shielding coil in this case is 539 V. Similarly for different locations of the shielding coils, the total magnetic field intensity is found to be reduced the most at 180 deg, which is the input voltage phase where the second term is the smallest.

2) S-S circuit

Fig. 10 shows the magnitude of each term in the S-S circuit when the shielding coil is installed next to the transfer coil. The total magnetic field strength is shown in Fig. 11. The input voltage to the transfer coil is 600 V and that to the shielding coil is 28 V.

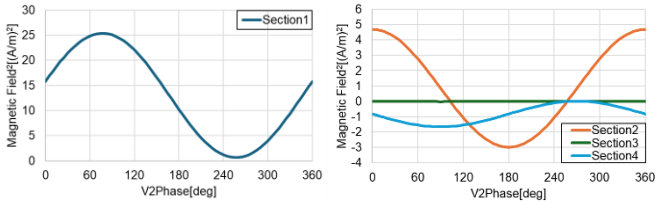

Fig.10 Comparison of magnitude for each term
(S-S, Shielding coil next to transfer coil)

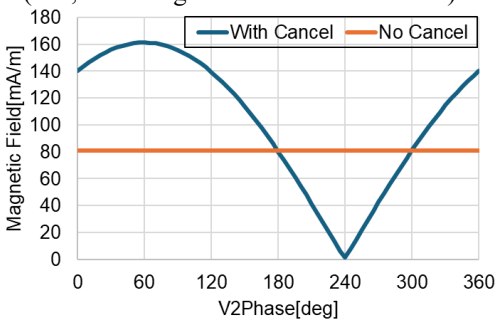

Fig.11 Magnetic field strength
(S-S, Shielding coil next to transfer coil)

From Fig.10, the magnitudes of the first and second terms change significantly when the input voltage phase to the shielding coil is changed. The absolute value of the first term is larger than that of the second term, indicating that the first term is dominant. From the above, Fig.11 shows that the leakage magnetic field is at its minimum at 240deg, which is slightly closer to the phase where the second term is at its minimum than the phase where the first term is at its minimum. Fig.12 shows the magnitude of each term and Fig.13 shows the total magnetic field intensity when the shielding coil is installed around the receiver coil. The magnitude of the input voltage to the shielding coil in this case is 678 V. When the location of the shielding coil is changed, only the second term changes significantly with the change of the input voltage phase to the shielding coil, and this term becomes dominant. Therefore, as shown in Fig.13, the leakage magnetic field is most reduced at 180 deg, where the second term is at its minimum.

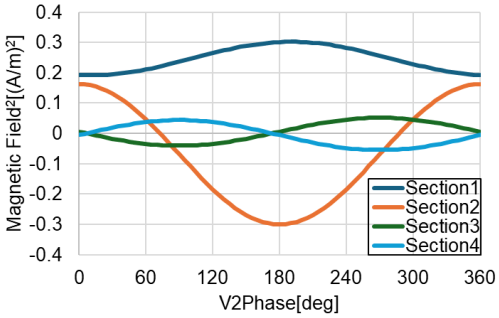

Fig.12 Comparison of the magnitude of each term
(S-S, Shielding coil around receiver coil)

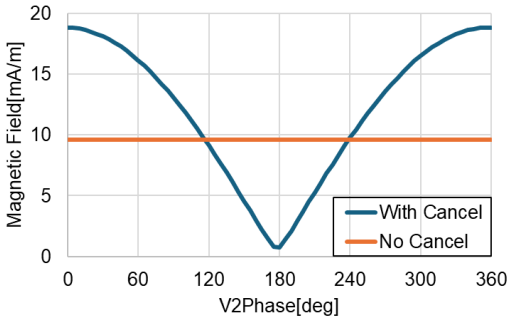

Fig.13 Magnetic field strength
(S-S, Shielding coil around receiver coil)

3) LCC-S circuit

In the LCC-S circuit, the magnitude of each term is shown in Fig. 14 when the shielding coil is installed next to the transfer coil. The total magnetic field strength is shown in Fig. 15. The input voltages to the transfer coil and shielding coil are 600 V and 587 V, respectively. Fig.14 shows that the second and fourth terms change when the phase of the input voltage to the shielding coil is changed. Among them, the change of the second term is larger and more dominant. From Fig.15, it is considered that the leakage magnetic field is at its minimum at 155 deg, which is closer to the phase where the fourth term is at its minimum than the phase where the second term is at its minimum.

Fig.16 shows the magnitude of each term and Fig.17 shows the total magnetic field intensity when the shielding coil is installed around the receiver coil. The magnitude of the input voltage to the shielding coil in this case is 543 V.

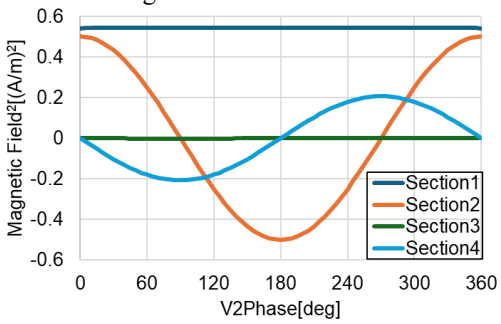

Fig.14 Comparison of magnitude for each term
(LCC-S, Shielding coil next to transfer coil)

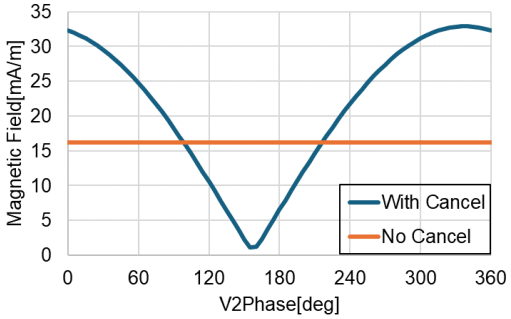

Fig.15 Magnetic field strength
(LCC-S, Shielding coil next to transfer coil)

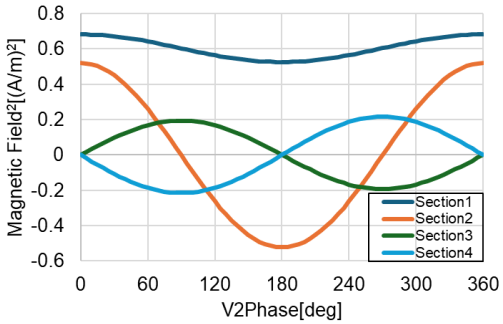

Fig.16 Comparison of the magnitude of each term
(LCC-S, Shielding coil around receiver coil)

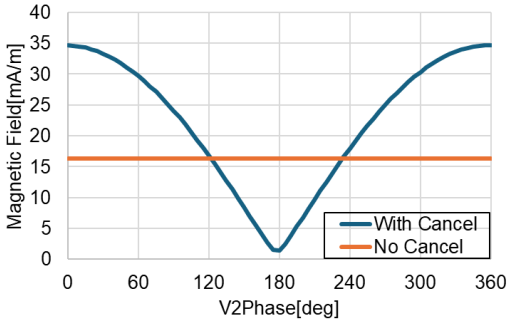

Fig.17 Magnetic field strength
(LCC-S, Shielding coil around receiver coil)

When the location of the shielding coil is changed, only the second term changes significantly with the change of the input voltage phase to the shielding coil, and this term becomes dominant. Therefore, as shown in Fig.17, the leakage magnetic field is most reduced at 180 deg where the second term is minimized. From the above, it can be said that for all three resonance methods, the leakage magnetic field reduction is largely affected by the phase difference between the transfer coil and the shielding coil.

V. Conclusion

A principle of leakage magnetic field reduction by adjusting the input voltage phase to the shielding coil was confirmed for an active shielding that uses a shielding coil to reduce the leakage magnetic field. When the input voltage phase to the shielding coil is changed, the current phase to the shielding coil changes, and the second term of equation (9) takes a large negative value, resulting in the magnetic field reduction. Phase difference between transfer coil and shielding coil causes leakage magnetic field reduction. The influence of the phase difference between the transfer coil and the receiver coil, and between the shielding coil and the receiver coil is negligible. It was found that the phase difference at this time was not optimal in reverse phase under all conditions, and that there were effects of the location of the shielding coil and the resonance method of the circuit. Even when other factors are considered, the second term of equation (9) is dominant, indicating the importance of adjusting the input voltage phase to the shielding coil in active shielding. In addition, the leakage magnetic field

strength is expressed in a form that is easy to calculate and can be used in the design of the WPT system.

ACKNOWLEDGMENT

This paper is based on results obtained from a project, JPNP21028, subsidized by the New Energy and Industrial Technology Development Organization (NEDO) in cooperation with DAIHEN Corporation.

REFERENCES

[1] SAE International, “Wireless Power Transfer for Light-Duty Plug-in/Electric Vehicles and Alignment Methodology J2954," Issued2016-05, Revised 2020-10.

[2] IEC International Electrotechinical Commission, "CiSPR 11 Consolida ted version," Jan 18, 2019 Publicated.

[3] B. S. Gu et al., "Optimisation of Magnetic Material Placement in IPT Pad for EV Charging," 2022 Wireless Power Week (WPW), Bordeaux, France, 2022, pp. 338-343

[4] P. Zhang, X. Yu, Q. Yang, X. Zhang, Y. Li and Z. Yuan, "Anti-saturation Shielding Coil with Coupling Enhancement for Wireless EV Charging," 2022 IEEE 20th Biennial Conference on Electromagnetic Field Computation (CEFC), Denver, CO, USA, 2022, pp. 1-2

[5] W. Lujun, Z. Yifan, C. Zhiwei, X. Xiaoming, D. Linzi and L. Hui, "Optimization of magnetic coupling shielding structure of DD coil for electric vehicle wireless charging based on parameter estimation," 2022 25th International Conference on Electrical Machines and Systems (ICEMS), Chiang Mai, Thailand, 2022, pp. 1-5

[6] J. Sun, R. Qin, J. Li, D. J. Costinett and L. M. Tolbert, "Design of a Resonant Reactive Shielding Coil for Wireless Power Transfer System," 2021 IEEE Applied Power Electronics Conference and Exposition (APEC), Phoenix, AZ, USA, 2021, pp. 1565-1572

[7] H. Kim, C. Song, J. Kim, J. Kim and J. Kim, "Shielded coil structure suppressing leakage magnetic field from 100W-class wireless power transfer system with higher efficiency," 2012 IEEE MTT-S International Microwave Workshop Series on Innovative Wireless Power Transmission: Technologies, Systems, and Applications, Kyoto, Japan, 2012, pp. 83-86

[8] Y. Wu, G. Zhang, Y. Wu, D. Zhang and L. Jing, "Research on Improving the Shielding Effect of Stacked Superconducting Bulks Based on Increasing the Gap Reluctance," in IEEE Transactions on Applied Superconductivity, vol. 33, no. 6, pp. 1-5

[9] S. Sato, Y. Tanaka, Y. Tsuruda and S. Nakamura, "Basic Investigation on Wireless Power Transfer System via Magnetic Resonant Coupling with Magnetic Field Suppression at an Any Point," IECON 2020 The 46th Annual Conference of the IEEE Industrial Electronics Society, Singapore, 2020, pp. 1555-1560

[10] J. Kim and S. Ahn, "Dual Loop Reactive Shield Application of Wireless Power Transfer System for Leakage Magnetic Field Reduction and Efficiency Enhancement," in IEEE Access, vol. 9, pp. 118307-118323, 2021

[11] A. D. Scher, M. Mohammad, B. Ozpineci and O. Onar, "Design and optimization of cancellation coil topologies for a ferrite-less wireless EV charging pad," 2021 IEEE Transportation Electrification Conference & Expo (ITEC), Chicago, IL, USA, 2021, pp. 1-7

[12] Y. Li, Y. Ying, K. Xie and S. Pan, "A Dual-Sided LCLC Topology for AGV Wireless Charging System With Low Leakage EMF," in IEEE Transactions on Electromagnetic Compatibility, vol. 65, no. 3, pp. 643-654, June 2023

[13] D. Kobuchi, K. Matsuura, Y. Narusue and H. Morikawa, "Magnetic Field Leakage Cancellation in Multiple-Input Multiple-Output Wireless Power Transfer Systems," in IEEE Magnetics Letters, vol. 13, pp. 1-4, 2022

[14] X. Zhang et al., "A Novel Hybrid Shielding Method With Single-Source Active Topology and Efficiency Stability for Wireless Power Transfer," in IEEE Transactions on Magnetics, vol. 59, no. 11, pp. 1-6, Nov. 2023

[15] M. Yokosawa et al., "Fundamental Study of Leakage Field Cancellation Coil Characteristics of Contactless Power-Feeding Coil for Power Feeding during Running," 2022 IEEE 7th Southern Power Electronics Conference (SPEC), Nadi, Fiji, 2022, pp. 1-6